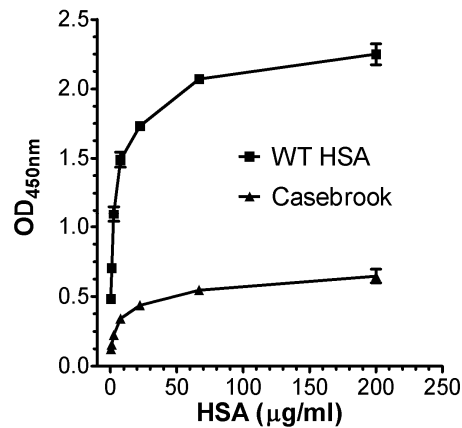
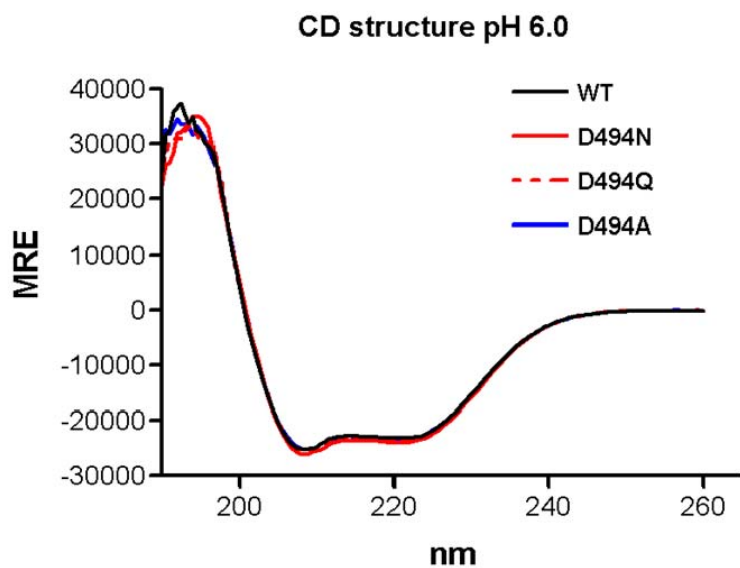


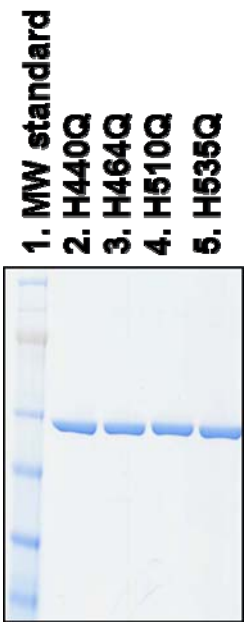
**Supplementary Figure S1. Binding of HSA mutants to hFcRn.** (a) The levels of titrated amounts of HSA variants (5.0-0.002 μg/ml) directly coated in the wells at pH 6.0 were controlled using a horseradish peroxidase conjugated anti HSA antibody preparation. ELISA responses of HSA WT, D494N, D494Q and D494A binding to hFcRn at (b) pH 6.0 and (c) pH 7.4. ELISA responses of HSA WT, D494N, D494N/T496A and T496A binding to hFcRn at (d) pH 6.0 and (e) pH 7.4. ELISA responses of HSA WT, E495Q and E495A binding to hFcRn at (f) pH 6.0 and (g) pH 7.4. In all FcRn binding experiments titrated amounts ( $100\text{-}0.4 \mu\text{g ml}^{-1}$ ) of the HSA variants were coated in wells followed by addition of a constant amount of hFcRn-GST ( $0.5 \mu\text{g ml}^{-1}$ ). Bound receptor was detected using an HRP-conjugated anti-GST antibody. The values represent the average of triplicates. (a-g)  $n=3\text{-}4$ . All data are presented as mean  $\pm$  s.d.



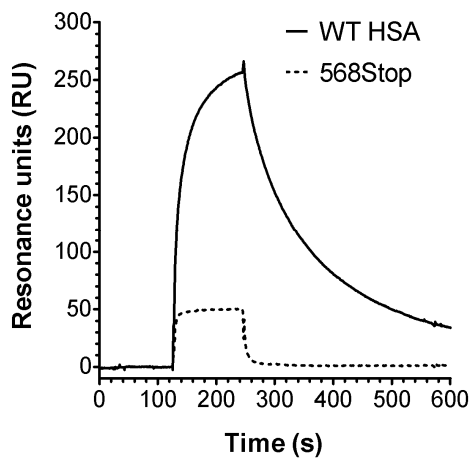
**Supplementary Figure S2. Binding of WT and Casebrook HSA to hFcRn.** ELISA responses showing binding of WT and the Casebrook HSA variant isolated from a heterozygous individual to hFcRn at pH 6.0. Titrated amounts of the HSA variants ( $200\text{-}0.3 \mu\text{g ml}^{-1}$ ) were coated in wells followed by adding of a constant amount of hFcRn-GST ( $0.5 \mu\text{g ml}^{-1}$ ). Bound receptor was detected using an HRP-conjugated anti-GST antibody. The values represent the average of triplicates.  $n=3$ . All data are presented as mean  $\pm$  s.d.



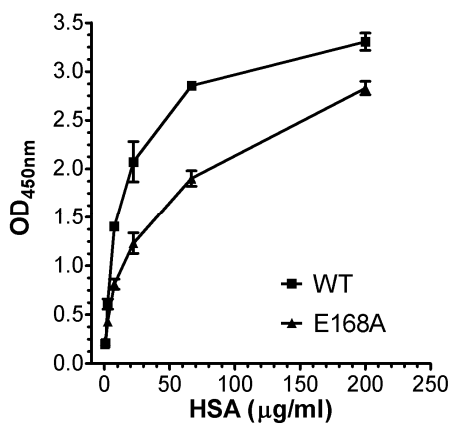
**Supplementary Figure S3. CD spectra for HSA variants.** Representative CD spectra of WT and HSA mutants obtained by CD measurements at pH 6.0. MRE; mean residual ellipticity. The secondary structural elements for each of the HSA variants are summarized in Supplementary Table S1.



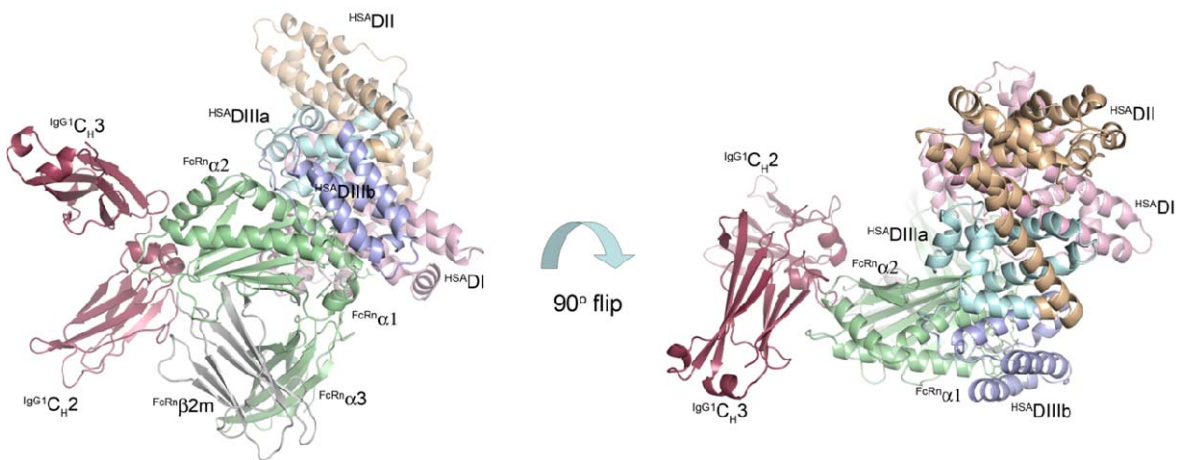
**Supplementary Figure S4. SDS-PAGE analysis of HSA variants.** Equal amounts (1 µg) of HAS variants (H440Q, H464Q, H510Q and H535Q) were applied on a NuPAGE 4-12% Bis-Tris gel. Electrophoresis was performed for 50 min at 200 V. Gels were stained with InstantBlue protein stain (Expedeon).



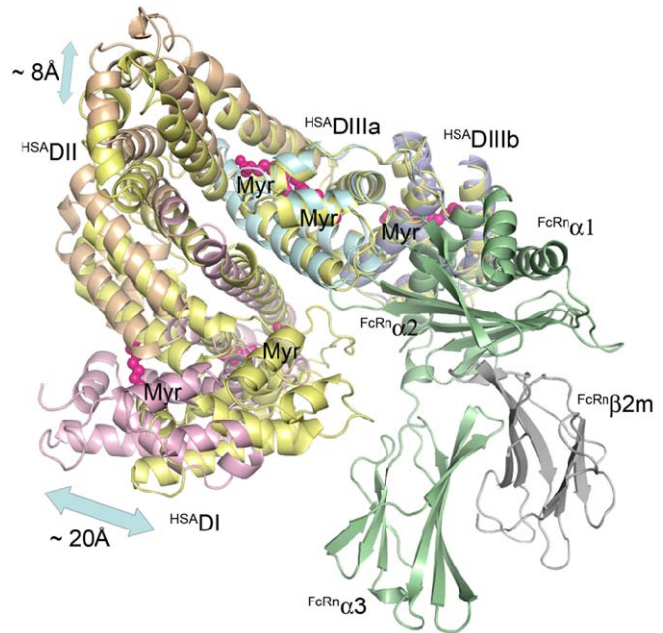
**Supplementary Figure S5. SPR binding responses of HSA variants.** Representative SPR responses obtained when 1  $\mu\text{M}$  of WT HSA and HSA 568Stop (truncated variant that lacks the last 17 a.a.) were injected over immobilized hFcRn (2000 RU) at pH 6.0. Injections were performed at 25 °C with flow rate of 50  $\mu\text{l min}^{-1}$ .



**Supplementary Figure S6. Binding of hFcRn variants to HSA.** ELISA responses showing binding of ( $0.5 \mu\text{g ml}^{-1}$ ) hFcRn WT and hFcRn E168A to titrated amounts of the WT HSA (200-0.3  $\mu\text{g ml}^{-1}$ ) coated in wells. The ELISA was performed at pH 6.0 and bound receptors were detected using an HRP-conjugated anti-GST antibody. The values represent the average of triplicates.  $n=3$ . All data are presented as mean  $\pm$  s.d.



**Supplementary Figure S7. A structural model of IgG and HSA bound to hFcRn.** The ternary model was made by superpositioning of the crystal structure of rat FcRn in complex with IgG2a Fc (Pdb code 1FRT) onto the hFcRn-HSA complex from the ZDOCK docking, followed by replacement of rat IgG2a Fc with the corresponding human IgG1 Fc (Pdb code 1l6x). The crystal model of the ternary hIgG1-hFcRn-HSA complex was designed using PyMOL (DeLano Scientific) and is shown in two orientations. The hFcRn HC in green,  $\beta$ 2m in gray, and the three HSA  $\alpha$ -helical domains DI in pink, DII in orange and DIII in cyan/blue. The HSA DIII is split into DIIIa (cyan) and DIIIb (blue). The two domains ( $C_H2$  and  $C_H3$ ) of half of the IgG1 Fc molecule are shown in maroon.



**Supplementary Figure S8. Predicted conformational change in HSA-hFcRn upon binding of fatty acids.** The docked HSA without fatty acids (yellow) binds to the  $\alpha 1$  and  $\alpha 2$  domains of hFcRn (green) mainly via HSA DIII and DI. Upon binding of fatty acids (5 myristate (Myr) molecules shown in magenta spheres), DI (pink) and DII (orange) undergoes a larger conformational change relative to DIII (cyan/blue), with up to 20 $\text{\AA}$  displacements. HSA DI moves away from hFcRn. The crystal structure figure was designed using PyMOL (DeLano Scientific) with the crystallographic data of HSA as previously described (Pdb codes 1bm0 and 1bj5). The hFcRn HC is shown in green and  $\beta 2\text{m}$  in gray.

**Supplementary Table S1. Secondary structural elements determined by CD**

HSA variant	Structural elements pH 7.4					Structural elements pH 6.0				
	Helix	Antiparallel	Parallel	Beta turn	Random coil	Helix	Antiparallel	Parallel	Beta turn	Random coil
<b>WT</b>	72	0	0,7	7,3	20	<b>64,8</b>	0,5	1,7	10,1	22,4
<b>D494N</b>	65,6	0,4	1,7	10,3	22	<b>67,9</b>	0,2	1,4	9,3	21,2
<b>D494A</b>	62,2	1,4	2,5	12,7	21,2	<b>65,9</b>	0,5	1,7	10,3	21,7
<b>E495Q</b>	65,3	0,3	1,7	10,4	22,2	<b>65</b>	0,6	1,8	10,5	22,1
<b>E495A</b>	64,8	0,5	1,8	10,6	22,2	<b>65,1</b>	0,5	1,7	10,5	22,2
<b>D494Q</b>	66,1	0,3	1,6	10,1	21,8	<b>67,1</b>	0,3	1,5	9,5	21,6

## Supplementary Table S2. CLUSTAL multiple amino acid alignment of albumin sequences

sheep	NLPPLTADFAEDKEVCKNYQEAKDVFGLGSFLYEYSRRPEYAVSVLLRLAKEYEATLEDC	359
goat	NLPPLTADFAEDKEVCKNYQEAKDVFGLGSFLYEYSRRPEYAVSVLLRLAKEYEATLEDC	359
cattle	NLPPLTADFAEDKEVCKNYQEAKDVFGLGSFLYEYSRRPEYAVSVLLRLAKEYEATLEEC	359
Donkey	DLPALAADFEDKEICKHYKDAKDVFLGTFLYEYSRRHPDYSVSLLLRIAKTYEATLEKC	359
Rabbit	GLPAVAEEFVEDKDVKKNYEEAKDLFLGKFLYEYSRRHPDYSVVLRLKGAYEATLKKC	360
mouse	DLPAIAADFVEDQEVCKNYAEAKDVFGLGTFLYEYSRRHPDYSVSLLRLAKKYEATLEKC	360
rat	DLPSIAADFVEDKEVCKNYAEAKDVFGLGTFLYEYSRRHPDYSVSLLRLAKKYEATLEKC	360
Hamster	DLPSLAADFVEDKEVCKNYAEAKDVFGLGTFLYEYARRHPDYSVALLRLAKKYEATLEKC	360
Guinea	ELPDLAVDFVEDKEVCKNFAEAKDVFGLGTFLYEYSRRHPESIGMLLRIAKGYEAKLEKC	360
	*** :: *.*.:::***: : *** *** *****:*****:***: :***:.* **:.*:*	
human	CAAADPHACYAKVDEFKPLVEEPQNLIKQNCELFEQLGEYKFQNALLVRYTKVPQVST	420
dog	CATDDPPCTCYAKVLDEFKPLVDEPQNLVKTNCFLFEKLGEYGFQNALLVRYTKAPQVST	420
sheep	CAKEDPHACYATVFDKLKHLDPEPQNLIKKNCFLFEKHGEYGFQNALLVRYTRKAPQVST	419
goat	CAKEDPHACYATVFDKLKHLDPEPQNLIKKNCFLFEKHGEYGFQNALLVRYTRKAPQVST	419
cattle	CAKDDPHACYSTVFDKLKHLDPEPQNLIKQNCDFEKLGEYGFQNALLVRYTRKVPQVST	419
Donkey	CAEADPPACAYATVFDQFTPPLVEEPKSLVKKNCFLFEVGEYDFQNALIVRVTKKAPQVST	419
Rabbit	CATDDPHACYAKVLDEFQPLVDEPKNLVQNCELYEQLGDYNFQNALIVRVTKKVPQVST	420
mouse	CAEANPPACYGTVLAEFQPLVVEEPKNLVKTNCFLFEYKLGEYGFQNAILVRYTQKAPQVST	420
rat	CAEGDPACYGTVLAEFQPLVVEEPKNLVKTNCFLFEYKLGEYGFQNAILVRYTQKAPQVST	420
Hamster	CAEADPSACYGKVLDEFQPLVVEEPKNLVKAANCELFEKLGEYGFQNALLVRYTQKAPQVST	420
Guinea	CAEADPHACYAKVFDLQPLIDEPKKLVQNCFLFDLGEYGFQNALLAVRYTQKAPQVST	420
	** :* * *.::: : *:***:.*: : *: : : *: ***: ****:*.*****	
human	PTLVEVSRNLGKVGSKCKHPEAKRMPCAEYLSSVVLNQLCVLHEKTPVSDRTVKCCTES	480
dog	PTLVEVSRKLGKVGTCKCKPESERMSCAEDFLSVLNRLCVLHEKTPVSEVRTKCCSES	480
sheep	PTLVEISRSLSLGKVGTCKCAKPESERMPCTEDYLSLILNRLCVLHEKTPVSEKVTKCCTES	479
goat	PTLVEISRSLSLGKVGTCKCAKPESERMPCTEDYLSLILNRLCVLHEKTPVSEKVTKCCTES	479
cattle	PTLVEVSRSLGKVGTCKCTKPESERMPCTEDYLSLILNRLCVLHEKTPVSEKVTKCCTES	479
Donkey	PTLVEIGRTLGKVGSRCKLPESERLPCSENHLALALNRLCVLHEKTPVSEKITKCCCTS	479
Rabbit	PTLVEISRSLSLGKVGSKCKHPEAERLPCVEDYLSVVLNRLCVLHEKTPVSEKVTKCCSES	480
mouse	PTLVEAAARNLGRVGTCKCTLPEAQRLPCVEDYLSAILNRVCCLHEKTPVSEHVTKCCSGS	480
rat	PTLVEAAARNLGRVGTCKCTLPEAQRLPCVEDYLSAILNRLCVLHEKTPVSEKVTKCCSGS	480
Hamster	PTLVEAARNLGVGSKCCVLPEAQRLPCVEDYISAILNRVCVLHEKTPVSEQVTKCCCTS	480
Guinea	PTLVEYARKLGSVGTCKCCSLPETERLSCCTENYLALILNRLCILHEKTPVSEVRTKCCTES	480
	***** .*.** ***:*** ** :*:.* *: : : *:***:*****:*****: *	
human	LVNRRPCFSALEVDETYVPKEFNAETFTFHADICTLSEKERQIKKQTAALVELVKHHPKAT	540
dog	LVNRRPCFSGLEVDETYVPKEFNAETFTFHADLCTLPEAEQVKKQTAALVELLKHHPKAT	540
sheep	LVNRRPCFSDTLDETYVPKPFDEKFTTFHADICTLPDETEQIKKQTAALVELLKHHPKAT	539
goat	LVNRRPCFSDTLDETYVPKPFDEGESFTFHADICTLPDETEQIKKQTAALVELLKHHPKAT	539
cattle	LVNRRPCFSALTPDETYVPKAFDEKLFTFHADICTLPDETEQIKKQTAALVELLKHHPKAT	539
Donkey	LAERRPCFSALELDEGYIPKEFKAETFTFHADICTLPDEDEQIKKQSAALELVVKHHPKAT	539
Rabbit	LVDRRPCFSALGPDETYVPKEFNAETFTFHADICTLPETERKIKKQTAALVELVKHHPKHAT	540
mouse	LVERRPCFSALTVDETYVPKEFKAETFTFHSDICTLPDEKEQIKKQTAALELVVKHHPKAT	540
rat	LVERRPCFSALTVDETYVPKEFKAETFTFHSDICTLPDEKEQIKKQTAALELVVKHHPKAT	540
Hamster	VVERRPCFSALPVDETYVPKEFKAETFTFHADICSLPEKEQMKKQAAALVELVKHHPKAT	540
Guinea	LVNRRPCFSALHVDETYVPKPFHADSFTFHADICTLPDEKEQVKKQMAVELVKHHPKAS	540
	: :***** * * * :*: * . . *:***:***:.*: : :***:***: ***.*:***:*	
human	KEQLKAVMDDFAAFVKECCKADDKETCFAAEGKKLVAASQAALGL 585	
dog	DEQLKTVMGDFGAFVKECCKAAENKEGCFSEEGPKLVAASQAALV- 584	
sheep	DEQLKTVMFVAFVDKCCAADDKEGCFVLEGPKLVASTQAALA- 583	
goat	DEQLKTVMFVAFVDKCCAADDKEGCFVLEGPKLVASTQAALA- 583	
cattle	EEQLKTVMFVAFVDKCCAADDKEACFAVEGPKLVVSTQTLA- 583	
Donkey	KEQLKTVLGNFSAFVAKCCGAADKEACFAVEGPKLVAASSQLALA- 583	
Rabbit	NDQLKTVVGFTALLDKCCSAEDKEACFAVEGPKLVESSKATLG- 584	
mouse	AEQLKTVMDFAQFLDTCKKAADKDTCFSTECPNLVTRCKDALA- 584	
rat	EDQLKTVMGDFAQFVDKCKKAADKDNCFATEGPNLVARSKEALA- 584	
Hamster	GPQLRTVLGEFTAFLDKCKKAEDKEACFSEDGPKLVASSQAALA- 584	
Guinea	EEQMKTVMGDFAAFLKKCCDADNEACFTEDGPKLVAKCQATLA- 584	
	* :***: * : : * * * : * : * : * : * : * : * :	

**Supplementary Table S3. HSA plasmids**

HSA mutein	Sub-cloning plasmid	Disintegration plasmid
Wild type	pDB2243	pDB2244
D494N	pDB3876	pDB3887
D494A	pDB3877	pDB3888
E495Q	pDB3878	pDB3889
E495A	pDB3879	pDB3890
D494Q	pDB3880	pDB3891
D494N, T496A	pDB3881	pDB3892
T496A	pDB3882	pDB3893

**Supplementary Table S4. HSA plasmids**

Amino acid substitution in HSA	Plasmid
HSA H440Q	pDB3986
HSA H464Q	pDB3987
HSA H510Q	pDB3988
HSA H535Q	pDB3989
HSA Q417A	pDB4084
HSA P499A	pDB4085
HSA K500A	pDB4086
HSA K536A	pDB4087
HSA P537A	pDB4088
HSA E501A	pDB4108
HSA K568*	pDB4557

\* = a stop codon was engineered into the DNA sequence encoding HSA to terminate the polypeptide sequence at amino acid 567.